

Prediction of Radiated EMI from Permanent Magnet Synchronous Motor Based on Field-circuit Coupled Method

Siqi Wei, Zeyu Pan, Jinghua Fan and Ping-An Du

Abstract—The Permanent magnet synchronous motor (PMSM) has been widely applied in a pulse width modulation inverter-fed adjustable speed drive (ASD) system. However, the radiated electromagnetic interference (EMI) from PMSM are proved to be non-negligible by experiments in radiated emission test. Since numerical methods in time domain have advantages in calculation electromagnetic fields over those in frequency domain. To this end the field-circuit coupled finite integral method in time domain is highly suggested to evaluate the radiated EMI from PMSM. In this paper, a simplified 3D EMI model of PMSM is developed and the current of motor windings, as the supply sources of radiated fields, are obtained by measurement. Besides, the field-circuit coupled method is employed to estimate the radiated EMI from PMSM. The effectiveness of the developed methodology is verified by implementation of experiments and simulation results show acceptable agreement with the experimental results.

Index Terms—radiated emissions, PMSM, electromagnetic interference (EMI), field-circuit coupled, finite integral-method

I. INTRODUCTION

DUE to its special merits of high power density as well as high torque density, the permanent magnet synchronous motor (PMSM), has been widely applied in pulse width modulation (PWM) inverter-fed adjustable speed drive (ASD) system.

Since the winding current of motor contains numerous harmonic components generated by the rapid changes in voltage (dv/dt) and current (di/dt) of the switching devices in an inverter, which acts as the major source for radiated EMI.

Manuscript received April 17, 2019; revised April 22, 2019. This work was supported by the National Natural Science Foundation of China under Grant 51675086.

Siqi Wei is currently a Ph.D. student at the University of Electronic Science and Technology of China, Chengdu, CO 611731 China (e-mail: weisqi0603@163.com).

Zeyu Pan is currently a master student at the UESTC, Chengdu, CO 611731 China (e-mail: panzeyuqingyu@139.com).

Jinghua Fan is currently a master student at the UESTC, Chengdu, CO 611731 China (e-mail: p15008488959@163.com).

Ping-An Du received the M.S. and Ph.D. degrees in mechanical engineering from Chongqing University, Chongqing, China, in 1989 and 1992, respectively. He is currently a full Professor of Mechanical Engineering at the University of Electronic Science and Technology of China, Chengdu, CO 611731 China (e-mail: dupingan@uestc.edu.cn). His research interests include numerical simulation in EMI, vibration, temperature, and so on.

The radiated EMI results from PMSM may leak through the gap of the motor shell, which may interfere with the performances of other electrical systems. According to the radiated emission test, the radiated EMI from PMSM is non-negligible, especially in electrical vehicles environment.

So far, extensive publications have discussed the conducted EMI issues in the motor drive systems and which clarified, in a certain extent, the characteristics of the conducted EMI researches [1]-[5]. Methods in both time and frequency domains have been presented to analyze the conducted EMI in ASD systems [6], [7]. The motor, involved in these studies, is considered as a load with its impedance equivalent by RLC elements for the conducted EMI circuit simulations. The studies of the radiated EMI concerning motors, however, are rarely made and only some low power DC motors are dealt with in literature [8]-[11]. The application of higher power motors in electric vehicles makes the radiated EMI from motors non-negligible within such a small confined space of vehicles.

Besides, the simplified lumped-circuit models are insufficient to take the place of Maxwell's equations while analyzing radiated emissions in a wide frequency band of concern, for the physical dimension of PMSM are not electrically small in consideration of frequencies more than 200MHz. The radiated EMI model of PMSM need to be suitable for both near field and far field analysis so as to according with electromagnetic compatibility (EMC) test standards such as CISPR25. Hence, the research on radiated EMI from PMSM deserves much more consideration to comply with rigorous governmental regulations on radiated emissions.

This paper presents a 3D full-wave model of PMSM to predict the radiated EMI based on the field-circuit coupled finite integral time-domain (FITD) method. The rest of this paper is organized as follows: introduction to the radiated EMI prediction methodology is shown in section II. Section III describes the radiated EMI model of PMSM. The experimental platform of the PMSM drive system is built in section IV to verify simulation results. Conclusions comes at the last in Section V.

II. THE PREDICTION METHODOLOGY OF RADIATED EMI

The computational process in frequency domain for obtaining radiation values within a certain frequency range is time consuming, which inspired the development of

methodologies in time domain [12]. One of industry standard software for 3D electromagnetic field analysis is CST (Computer Simulation technology) from SIMULIA. FITD was firstly proposed by Weiland in 1976/1977 [13]. This numerical method discretizes the following integral form of Maxwell's equations:

$$\oint_{\partial A} \vec{E} \cdot d\vec{s} = - \int_A \frac{\partial \vec{B}}{\partial t} \cdot d\vec{A} \quad (1) \quad \oint_{\partial A} \vec{H} \cdot d\vec{s} = \int_A \left(\frac{\partial \vec{D}}{\partial t} + \vec{J} \right) \cdot d\vec{A} \quad (2)$$

$$\oint_{\partial V} \vec{D} \cdot d\vec{A} = \int_V \rho dV \quad (3) \quad \oint_{\partial V} \vec{B} \cdot d\vec{A} = 0 \quad (4)$$

The spatial discretization Maxwell's equations are formulated for the hexahedral grid cells and then the complete discretized set of Maxwell's Grid Equations (MGEs) are obtained by applying Faraday's Law and Ampère's law in each of the cell facets. Since the set of MGEs maintain energy and charge conservation, FITD method affected-free by such problems, that is, the spatial discretization of a numerical algorithm could cause long-term instability [14]-[16].

The field-circuit coupled method has been put forward to build the EMI prediction model of motors. Fig.1 shows the implementation of the radiated EMI prediction procedure based on field-circuit coupled FITD method. Firstly, a 3D motor model with discrete ports is built in the CST Microwave studio (MWS). Afterwards, excitation sources are fed into 3D structure via discrete ports which are automatically generated in circuit model. And lastly, the radiated EMI from motor is computed by applying 3D field-circuit co-simulation.

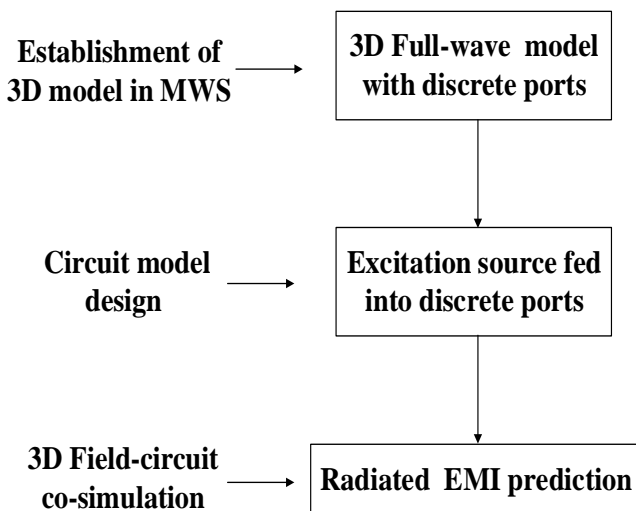


Fig. 1. Implementation procedure for the radiated EMI prediction model.

The motor winding currents, as the excitation sources for simulation, are measured under no-load working condition of motor by a current probe (TCP0150) from Tektronix Inc. The measured three-phase currents are shown in Fig. 2. It is illustrated that three-phase currents obtained by PWM contain a number of harmonic components. The current waveforms are approximately sinusoidal.

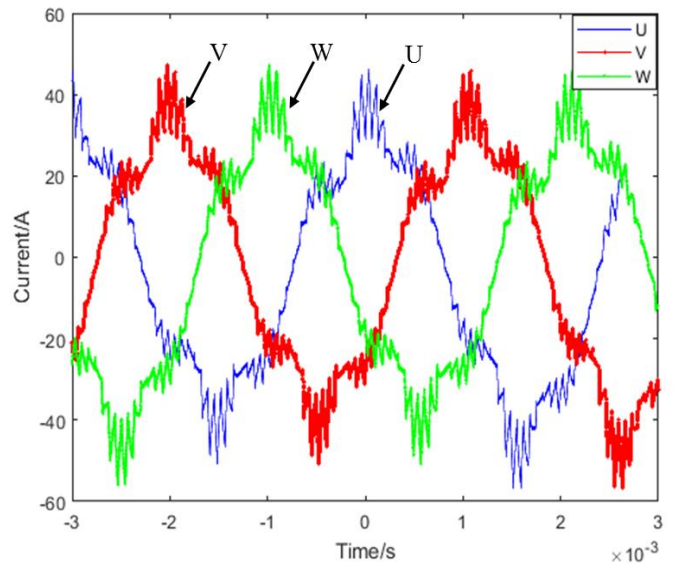


Fig. 2. Measured three-phase currents by current probe TCP0150.

III. RADIATED EMI MODEL DESCRIPTION

A. Motor

The 3D motor model is established in accordance with its actual geometry. The detailed design parameters are listed in Table I.

TABLE I
SPECIFICATIONS OF THE PMSM

Item	Value
Rated power	4kW
Rated speed	3000rpm
Number of stator slots	12
Number of poles	8
Stator outside radius	73mm
Stator inside radius	45.6mm
Rotor outside radius	44.25mm
Rotor inside radius	15.12mm
Axial length	102mm
Magnet material	Nd-Fe-B
Motor shell material	Al-alloy
Stator and rotor core material	DW465_50

The simplification on the motor model is considered motivated by uneasiness of removing limitations of computer capabilities. The motor shell, for instance, is simplified to a cylinder, due mainly to grooves on the surface of a motor shell is only to expand the heat dissipation area and have little effect on the calculation of radiation EMI. When modeling the shell or other trivial parts of motor with their actual structure, the total number of grids which are subjected to the minimum size of structure will increase tremendously. This is quite impossible to employ numerical simulation depending on the limited hardware capabilities. Consequently, small structures with little effect in radiated emissions are not taken into account in the motor 3D model. The simplified 3D motor model is shown in Fig. 3.

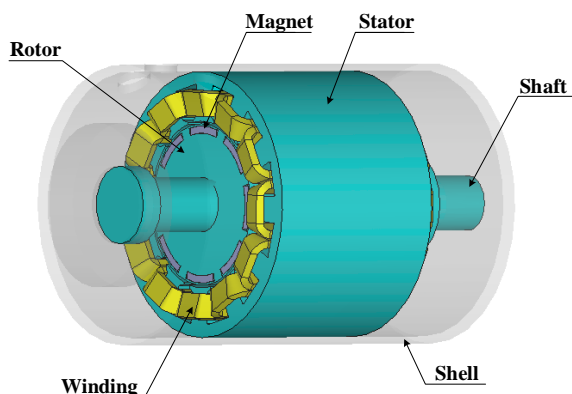


Fig. 3. Simplified 3D Full-wave model of the PMSM.

B. Ground

The motor is usually fixed to the frame (ground). Similarly, in experiments of EMC test, the motor is placed on the metal plate of the test table which is regarded as a reference ground plane. In order to have an identical configuration for both simulation and experiment, a ground model with the same size as the test table is determined as 250mm x 150mm x 2mm, illustrated in Fig. 4.

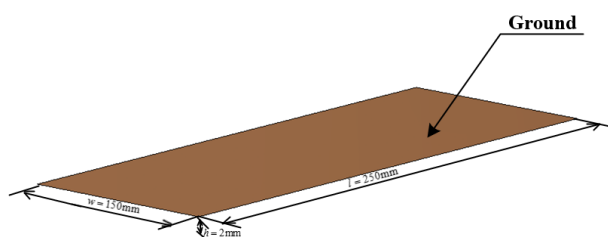


Fig. 4. The CAD model of the ground.

C. Excitation sources

Twelve discrete ports are defined in each single coil of motor windings in the 3D model. These discrete ports designed in MWS can automatically generate 12 connection ports when converted to the circuit design model as shown in Fig. 5. A transient simulation task is set up to import the measured three-phase current into the circuitry as excitation sources. The excitation sources are then fed into the motor windings by matching with discrete ports in sequence for carrying out field-coupled co-simulation ultimately.

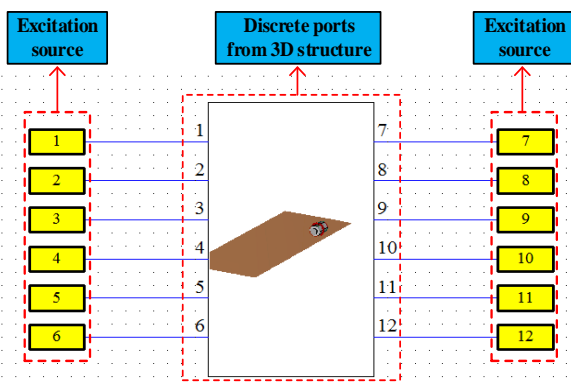


Fig. 5. Excitation sources added in the circuit design model.

IV. SIMULATION AND EXPERIMENTAL RESULTS

A motor driving system for experiment is established to verify the radiated EMI prediction results. The system consists of a power supply, a PWM inverter, three-phase cables, DC cables and a PMSM. The schematic of the system is shown in Fig. 6.

A metal netting connected to the ground is utilized for shielding radiated electric field from the devices except for line impedance stability network (LISN) and PMSM. The receiving antenna is placed at a distance of one meter from the center of three phase cables. An electric field probe is set up in the simulation model to monitor the radiated emissions at the same location. The PWM inverter in this system is powered by 60V DC voltage. Additionally, in the experiment, the motor under no-load working condition is assumed to operate at a constant speed of 4600rpm. The experiment bench is set as shown in Fig. 7.

A monopole antenna is employed to measure emissions from 10 kHz to 30 MHz for the vertical polarization and a bi-conical antenna is used to measure emissions from 30 MHz to 200 MHz for both horizontal and vertical polarization. Modifying factors of antenna at different frequencies are compensated directly by EMI receiver. The comparison between the measured and simulated emissions in the frequency range from 10 kHz to 30 MHz and that from 30 MHz to 200 MHz at one meter away from the edge of the reference ground are shown in Fig. 8 and Fig. 9, respectively.

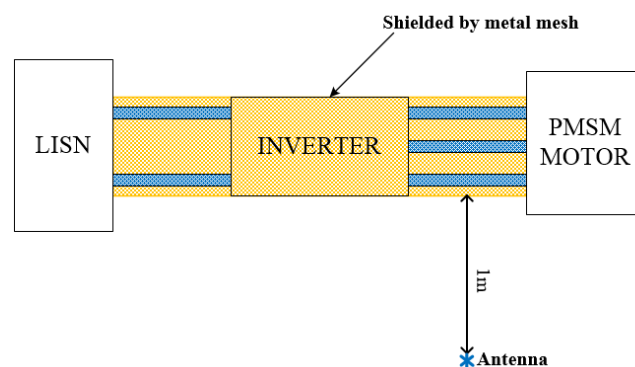


Fig. 6. Schematic of a motor drive system for radiated EMI measurements.



Fig. 7. Experiment bench of an ASD system based on PMSM

The predicted and experimental electric fields for the vertical polarization in the 10 kHz to 30 MHz frequency range show a good agreement. In the range of 30 MHz to 200 MHz frequency, for the vertical polarization, the proposed method predicts the radiation trend of electric field well. Though in the 30 MHz to 200 MHz frequency range for the horizontal

polarization, there are distinct discrepancies between the predicted fields and that from measurements. The reason for such discrepancies is the radiated emissions are affected considerably by the reflection of the metal shielded netting in the horizontal direction than the vertical during the experiments.

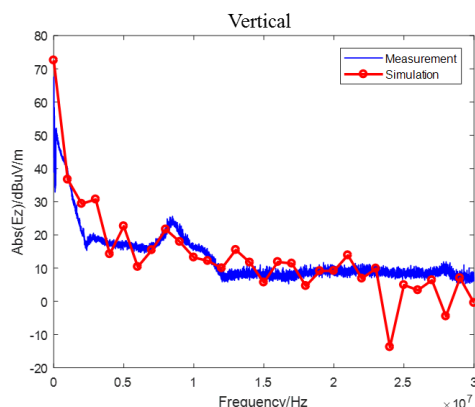


Fig. 8. Comparison between the measured and simulated radiated EMI in the 10 kHz to 30 MHz frequency range.

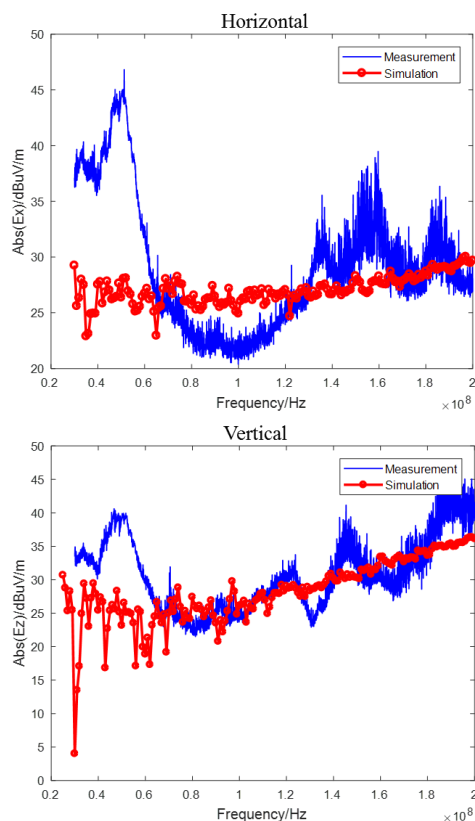


Fig. 9. Comparison between the measured and simulated radiated EMI in the 30 MHz to 200 MHz frequency range.

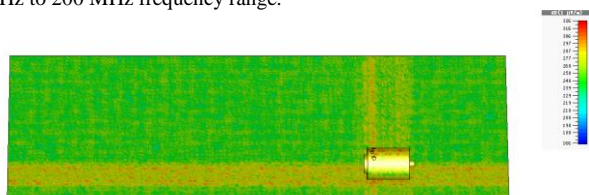


Fig. 10. The electric field snapshot in vertical direction at $t=1\mu s$

The electric field snapshot in vertical direction at $t=1\mu s$ is obtained, which gives a visual interpretation of propagation of wave from PMSM, shown in Fig. 10.

Particularly, four probes in a horizontal plane at the same height, as shown in Fig. 11, are arranged to investigate locations that are more susceptible to the radiated EMI from PMSM. Every probe is at an equal distance from the central position of motor which is as the origin of a reference coordinate. Simulation results with four coordinate values are illustrated in Fig. 12.

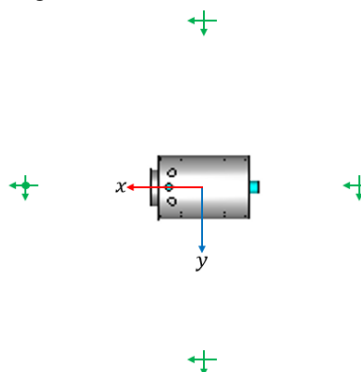


Fig. 11. Four probes set up in the same horizontal plane.

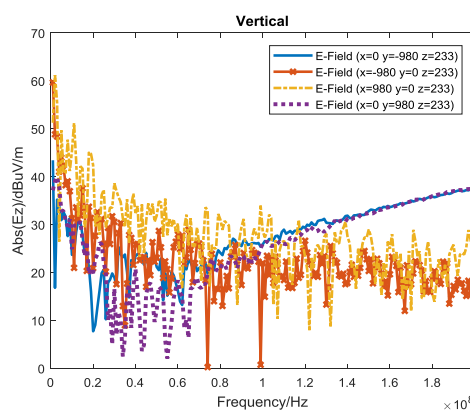


Fig. 12. Simulated radiated EMI results of four probes in different directions from 10 kHz to 200MHz.

It can be seen that the radiated EMI in Y direction from motor is much stronger than that in X direction when the frequency is more than 150MHz. That means other electronic equipment which exhibits high susceptibility in the 150 MHz to 200 MHz frequency range should be better positioned in X direction of motor rather than Y for immunity from external disturbances.

V. CONCLUSION

The prediction of radiated EMI from PMSM based on field-coupled FIT method is concluded by the proposed methodology which is validated by experiments in this paper. The developed methodology offers a new means of looking inside the radiated emissions from motor, which is referential to other electromechanical equipment containing high-frequency current sources. Some guidelines are able to get for optimizing the overall layout with other power electronics equipment by simulation. The prediction method is profitable to suppress electromagnetic interference from motors in the engineering design stage and improve EMC in the system-level.

REFERENCES

- [1] Gubia, E., Sanchis, P., Ursua, A., Lopez, J., & Marroyo, L. . "Frequency domain model of conducted EMI in electrical drives," *IEEE Power Electronics Letters*, vol. 3, no. 2, pp. 45–49, 2005.
- [2] H. Zhu, J.-S. Lai, Y. Tang, A. Hefner, Jr. D. Berning and C. Chen "Analysis of conducted EMI emissions from PWM Inverter based on empirical models and comparative experiments," in *Conf. Rec. of IEEE Power Electronics Specialists Conference.*, June 1999, pp. 111–123.
- [3] H. Zhu, Jih-Sheng Lai, A. R. Hefner, Jr., Y. Tang, and C. Chen, "Modeling based examination of conducted EMI emission from hard and soft-switching PWM inverters," *IEEE Transactions on Industry Applications*, Sep./Oct., 2001, pp. 1383–1393.
- [4] Nave, Mark J. "Prediction of conducted emissions in switched mode power supplies," *IEEE International Symposium on Electromagnetic Compatibility*, 1986, pp. 1-7.
- [5] Chen, Chingchi, X. Xu, and D. M. Divan. "Conductive electromagnetic interference (EMI) noise evaluation for an actively clamped resonant DC link inverter (ACRDCLI) for electric vehicle (EV) traction drive applications." *Conference Record of the 1997 IEEE Industry Applications Conference Thirty-Second IAS Annual Meeting*, vol. 2, pp. 1550-1557, 1997.
- [6] Ran, L., Gokani, S., Clare, J., Bradley, K. J., & Christopoulos, C. "Conducted electromagnetic emissions in induction motor drive systems. I. Time domain analysis and identification of dominant modes," *IEEE Transactions on Power Electronics*, vol. 13, no. 4, pp. 757–767, 1998.
- [7] Ran, L., Gokani, S., Clare, J., Bradley, K. J., & Christopoulos, C. "Conducted electromagnetic emissions in induction motor drive systems. II. Frequency domain models," *IEEE Transactions on Power Electronics*, vol. 13, no. 4, pp. 768–776, 1998.
- [8] Huangfu, Y., Wang, S., Di Rienzo, L., & Zhu, J. "Radiated EMI modeling and performance analysis of a PWM PMSM drive system based on field-Circuit coupled FEM," *IEEE Transactions on Magnetics*, vol. 53, no. 11, pp. 1–4, 2017.
- [9] Suriano, C. R., Suriano, J. R., Thiele, G., & Holmes, T. W. "Prediction of radiated emissions from DC motors," In *1998 IEEE EMC Symposium, International Symposium on Electromagnetic Compatibility. Symposium Record*, vol. 2, pp. 790-795, August.1998.
- [10] Motter, D. P. "Commutation of DC machines and its effects on radio influence voltage generation," *Transactions of the American Institute of Electrical Engineers*, vol. 68, no. 1, pp.491–496, 1949.
- [11] J. Sach, H. Schmeer. "Computer aided analysis of RFI voltage generation by small commutate motors," *Symposium and Technical Exhibition on Electromagnetic Compatibility*, no. 6, Zurich, 1985, pp. 551–556.
- [12] Jin, Jianming. *The Finite Element Method in Electromagnetics. The Finite Element Method in Electromagnetics, 2nd Edition*. 2002.
- [13] Weiland, T. "A discretization model for the solution of Maxwell's equations for six-component fields," *Archiv Elektronik Und Uebertragungstechnik*, no. 31, pp. 116–120, 1977.
- [14] Weiland, T. . "Time domain electromagnetic field computation with finite difference methods," *International Journal of Numerical Modelling Electronic Networks Devices & Fields*, vol. 9, no. 4, pp. 295–319, 2015.
- [15] Clemens, M. , and T. Weiland . "Discrete electromagnetism with the finite integration technique – abstract," *Journal of Electromagnetic Waves and Applications*, vol. 15, no. 1, pp. 79–80, 2001.
- [16] Weiland, Thomas. "RF & microwave simulators: from component to system design," *IEEE European Microwave Conference*, 2003, pp. 591-596.